Green Chemistry

PAPER

View Article Online
View Journal

Cite this: DOI: 10.1039/c6gc00883f

Direct C–C coupling of bio-ethanol into 2,3-butanediol by photochemical and photocatalytic oxidation with hydrogen peroxide†

Na Li,[a] Wenjun Yan,[a] Pengju Yang,[a,b] Hongxia Zhang,[a,c] Zhijian Wang,[a] Jianfeng Zheng,[a] Suping Jia[a] and Zhenping Zhu*[a]

Received 29th March 2016,
Accepted 14th June 2016

DOI: 10.1039/c6gc00883f

www.rsc.org/greenchem

Theoretically, selective C–H manipulation in ethanol can result in a direct C–C coupling synthesis of 2,3-butanediol (2,3-BDO). However, this process is typically extremely difficult to achieve because of the high complexity of the involved chemical bonds. In this work, we determine that hydroxide radicals generated from the photolysis of H_2O_2 can selectively attack the α-hydrogen atom in ethanol aqueous solutions and crack the C–H bond to produce hydroxyethyl radicals, which subsequently undergo C–C coupling to form 2,3-BDO. This selective C–H breakage is determined by the reaction rate, which is primarily controlled by the local H_2O_2 concentration at a given irradiation intensity. At a moderate reaction rate of ethanol (37 mmol h^{-1}), the 2,3-BDO selectivity reaching as high as 91% can be obtained. The introduction of a catalyst can further increase ethanol conversion and enhance the 2,3-BDO formation rate by controlling the reaction rate. This result provides an environment-friendly approach to convert bio-ethanol directly to 2,3-BDO and to manipulate a single bond selectively in complex bonding situations.

Introduction

In the modern green chemical industry, selectively manipulating chemical bonds is a primary approach in organic chemistry and catalysis science that is becoming increasingly important.[1] Among them, the practical and selective functionalization of traditionally inert aliphatic C–H bonds has been developed as a powerful strategy to form new chemical bonds.[2,3] However, one of the major challenges facing the continued advance of this field is the ability to manage a single bond controllably in a compound containing many such bonds and an array of functional groups.[4] With the increasing demands for energy, concerns about anthropogenically caused global climate change, and depletion of fossil feedstock, more and more attempts have been focusing on alternative and renewable biomass sources for fuels and chemicals. Bio-ethanol, as an important biomass platform molecule, has great potential as a renewable alternative to petroleum, with the advantage of being compatible with the current infrastructure.[5] In the past decade, bio-ethanol production rapidly increased and the total annual capacity reached 100 billion L in 2013.[6] The transformation of bio-ethanol into valuable chemicals or high calorific value fuels is of great interest in different countries owing to its availability as a feedstock. However, some limitations need to be overcome for the effective application of bio-ethanol. For example, bio-ethanol obtained by fermentation of biomasses has large amounts of water (12% ethanol) and its dehydration is very complex requiring the consumption of large amounts of energy with a higher cost due to ethanol–water azeotropic solution.[7,8] From the economic standpoint, development of the water phase reaction for ethanol conversion is very profitable. Moreover, ethanol has multifarious chemical bonds, including α-C–H, β-C–H, O–H, C–O, and C–C. These bonds provide ethanol with versatile functional properties, which has resulted in the current extensive ethanol industry that produces aldehydes, acids, ethers, esters, olefins, *etc.*[9] However, it is difficult to selectively cleave C–H bonds to form new C–C bonds, which is important and challenging in increasing the conversion efficiency and purity. Wang *et al.* found that the initial dissociation step of ethanol prefers to begin with its O–H bond cleavage leading to CH_3CH_2O and H species rather than the cleavage of other bonds.[10] Davis *et al.* reported the coupling reaction of ethanol into butanol over hydroxyapatite and magnesia, and the products formed are ethane and acetaldehyde in addition to butanol.[11] The direct transformation of ethanol into ethyl acetate through acetaldehyde formation

---

[a] *State Key Laboratory of Coal Conversion, Institute of Coal Chemistry, Chinese Academy of Sciences, Taiyuan, 030001 Shanxi, China. E-mail: zpzhu@sxicc.ac.cn*
[b] *Graduate University of Chinese Academy of Sciences, Beijing 100039, China*
[c] *Institute of Application Chemistry, shanxi University, Taiyuan 030001, China*

† Electronic supplementary information (ESI) available. See DOI: 10.1039/c6gc00883f

with bimetallic Pd/Zn catalytic membrane reactors was reported. In this process, the main job was how to avoid the transformation of ethanol to CO and CH_4.[12] Thus, it is very difficult to effectively and selectively cleave C–H bonds of ethanol because two or more bonds may be broken simultaneously.

2,3-BDO is a versatile platform chemical and a potential aviation fuel with a high calorific value (27 198 J g^{-1}), which can be used to produce butadiene (a monomer of synthetic rubber), methyl ethyl ketone (an excellent organic solvent for resins and lacquers), acetoin, and diacetyl (a flavor enhancer) through a dehydration or dehydrogenation reaction.[13–15] The increasing annual demand for 2,3-BDO has become a valuable commercial opportunity.[16] Generally, 2,3-BDO could be produced from carbohydrates (glucose, sucrose, glycerol *etc.*) by a bacterial fermentation pathway. So far, the generation rate of 2,3-BDO from glucose is higher than other carbon sources, which is not ideal for industrial production.[17,18] Moreover, large-scale commercial production of 2,3-BDO using bacterial fermentation might be difficult in terms of safety regulations and the high cost of the feedstock.[19–21] Thus, developing a green, clean and high efficiency process based on using low-cost and renewable resources as substrates is imperative.

In this work, we reported the one-step synthesis of 2,3-BDO from bio-ethanol *via* the C–C coupling reaction at room temperature. In this process, we found that hydroxyl radicals generated from the photolysis of H_2O_2 under UV irradiation can selectively attack the α-hydrogen atom in ethanol aqueous solutions and crack the α-C–H bond to produce hydroxyethyl radicals ($^{\bullet}CH(OH)CH_3$), which subsequently undergo C–C coupling to form 2,3-BDO. At a moderate ethanol reaction rate (37 mmol h^{-1}), the 2,3-BDO selectivity can reach as high as 91%. Suzuki *et al.* also described the laser-induced selective synthesis of diols from methanol and ethanol in the presence of H_2O_2.[22] When ethanol was irradiated, the products were acetaldehyde and butanediol (including 2,3-, 1,3- and 1,4-butanediol). Acetaldehyde was the major product and the selectivity was as high as 62%, which showed that the O–H bond scission was the main in this process, consistent with the report of Wang *et al.*.[10] Moreover, the selectivities of butanediol *e.g.* 2,3-, 1,3-, and 1,4-butanediol were 29%, 1%, and 2%, respectively. For diols, they found that hydroxyl radicals competitively attacked α-C–H and β-C–H of ethanol to form α-hydroxyethyl radicals ($^{\bullet}CH(OH)CH_3$) and β-hydroxyethyl radicals ($^{\bullet}CH_2CH_2OH$), which subsequently dimerized to form 2,3- and 1,4-butanediol. However, the selectivity of diols was extremely low at 29%, which demonstrates that this technology is unsuitable for precisely manipulating single α-C–H bond breakage. In comparison with the report of Suzuki *et al.*, our advantages were mainly manifested on the following two aspects: (1) selectively manipulating α-C–H of ethanol: the hydroxyl radicals can selectively break the α-C–H of ethanol to form a new C–C bond, which can be demonstrated by EPR and the high selectivity of 2,3-BDO (91%). Moreover, other butanediols (*e.g.* 1,4 or 1,3-butanediol) were not detected in our experiment. (2) Bio-ethanol instead of ethanol as the raw material: we choose water as the solvent to avoid the elimination of extensive water in bio-ethanol, which increases the availability and decreases the cost. For increasing the ethanol conversion rate, we investigated the influence of some catalysts on the C–C coupling reaction efficiency. From the experiment, we observe that the introduction of a catalyst can further accelerate ethanol conversion and enhance the formation rate of 2,3-BDO by controlling the reaction rate. This result not only indicates the practical possibility of directly coupling bio-ethanol into diols but also demonstrates how a single bond in a complex bonding circumstance can be precisely manipulated.

Results and discussion

To validate the selectivity of H_2O_2 in attacking the chemical bond of ethanol in aqueous solutions, the electron paramagnetic resonance (EPR) spin trapping technique was used. The reaction of H_2O_2 with bio-ethanol under UV irradiation *in situ* was investigated. The 5,5-dimethyl-l-pyrroline N-oxide (DMPO) spin trap was used in these experiments to detect radical intermediates. As shown in Fig. 1A, a four-line EPR signal from an apparent hydroxyl radical adduct with DMPO (DMPO/$^{\bullet}$OH, $a_N = a_H = 14.47$ G), which was formed by the photolysis of H_2O_2, could be observed. Furthermore, the other six-line EPR signal was characteristic of DMPO/$^{\bullet}CH(OH)CH_3$ with a_N = 15.8 G and a_H = 22.6 G, which was the result of the abstraction of the α-hydrogen atom of ethanol by $^{\bullet}$OH. Fig. 1 (curve b) shows the computer simulation of the experimental spectrum at the third minute of illumination based on the coupling constants given for the DMPO spin adducts of $^{\bullet}CH(OH)CH_3$ and $^{\bullet}$OH radicals. On the basis of the intensity ratio of these two adducts (9 : 1), we confirmed that $^{\bullet}CH(OH)CH_3$ was the major intermediate radical for the reaction system. This result suggests that the hydroxyl radical from the photolysis of H_2O_2 can precisely crack the α-C–H of ethanol aqueous solutions into the $^{\bullet}CH(OH)CH_3$ radical.

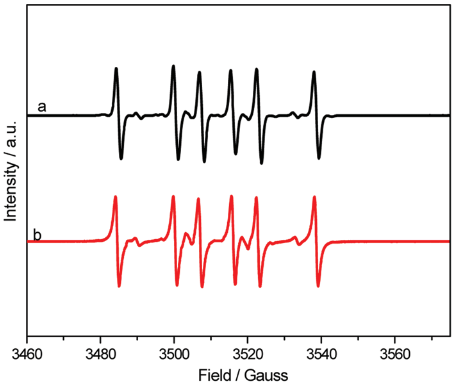

Fig. 1 EPR spectrum of the $CH_3CH_2OH–H_2O–H_2O_2$–DMPO system at the third minute of illumination. (a) Experimental spectrum; (b) spectrum for computer simulation with two species: I, DMPO/OH; $a_N = a_H$ = 14.47 G II, DMPO/$CH(OH)CH_3$ with a_N = 15.8 G and a_H = 22.6 G.

Moreover, we performed the photochemical C–C coupling reaction in a 200 mL aqueous solution under an argon atmosphere under UV irradiation at room temperature. The initial concentration of ethanol was 2.39 mol L^{-1}, whereas that of H_2O_2 was 0.25 mol L^{-1}. 2,3-BDO was produced as a major product, whereas acetaldehyde, acetic acid, carbon dioxide, carbon monoxide and methane were the minor products.

The conversion of ethanol was 14.2%, and the selectivity of 2,3-BDO was 84% after 5 h (Fig. 2). On the basis of these preliminary data, 2,3-BDO could be selectively produced through the C–C coupling of bio-ethanol. We examined the photolysis of H_2O_2, the conversion of ethanol, and the selectivity of products as a function of reaction time. As shown in Fig. 2A, the photolysis rate of H_2O_2 was extremely rapid in the beginning. However, as the reaction time increased, the photolysis rate slowed down and the concentration of H_2O_2 decreased in the solution. The conversion of ethanol is basically consistent with the photolysis of H_2O_2. When the photolysis rate is fast, the quantity of $^{\bullet}OH$ is large, and the conversion of ethanol is high. When H_2O_2 decomposed completely, the conversion of ethanol approached equilibrium for approximately 5 h. As shown in Fig. 2B, the selectivity of excessive oxidation products, namely, acetaldehyde and acetic acid, were high at the initial reaction stage. By contrast, the selectivity of 2,3-BDO was low. As the reaction progressed, the selectivity of acetaldehyde and acetic acid evidently reduced, whereas the selectivity of 2,3-BDO gradually increased and then leveled off. The gas products, namely, CO, CO_2, and CH_4, did not evidently change in the entire reaction process. This outcome could be attributed to the high concentration of H_2O_2 that produced a large amount of $^{\bullet}OH$ during the early stage, which could not only attack the α-C–H of ethanol to form $^{\bullet}CH(OH)CH_3$ radicals, but could also further break down the other O–H, C–O, and C–C bonds of ethanol to form aldehydes, acids, or even CO_2. With the increment of time, the H_2O_2 concentration and the decomposition rate decreased to produce moderate $^{\bullet}OH$ radicals, which preferentially manipulated the α-C–H bond of ethanol in aqueous solutions. Thus, the selectivity of 2,3-BDO improved eventually. When $^{\bullet}OH$ disappeared, the quantity of 2,3-BDO became approximately constant.

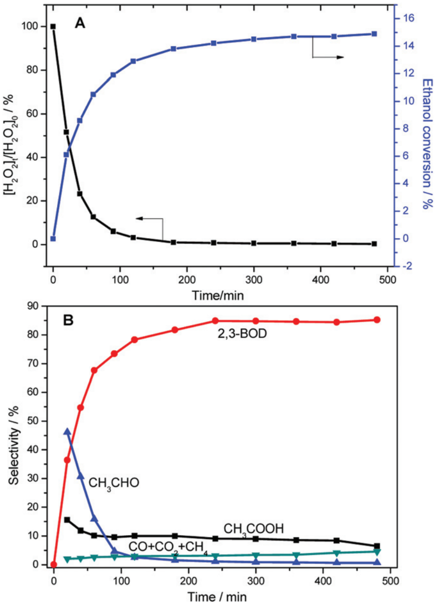

Fig. 2 (A) The conversion of ethanol and the photolysis of H_2O_2 as a function of the reaction time. (B) The selectivity of products as a function of the reaction time (conduction: ethanol 0.479 mol, H_2O_2 (30%) 0.05 mol, 200 ml; 300 W high pressure Hg lamp).

From the preceding data, we conjectured that H_2O_2 concentration might be one of the important factors that controlled the selectivity of 2,3-BDO. Thus, a series of comparative experiments was performed using a 2.4 mol L^{-1} ethanol aqueous solution with different H_2O_2 initial concentrations under a 300 W high-pressure mercury vapor lamp for 5 h. Moreover, the utilization efficiency of H_2O_2 was also investigated through comparative experiments, which can reflect how much H_2O_2 was used for effective coupling of bio-ethanol to 2,3-BDO, because the $^{\bullet}OH$ from the photolysis of H_2O_2 can not only crack the α-C–H bond to produce $^{\bullet}CH(OH)CH_3$ (eqn (1)–(3)), but can also cause a chain self-decomposition reaction with residual H_2O_2 to form O_2 (eqn (4) and (5)).

$$H_2O_2 + h\nu \rightarrow {}^{\bullet}OH \tag{1}$$

$${}^{\bullet}OH + CH_3CH_2OH \rightarrow {}^{\bullet}CH(OH)CH_3 + H_2O \tag{2}$$

$$2{}^{\bullet}CH(OH)CH_3 \rightarrow CH_3CH(OH)CH(OH)CH_3 \tag{3}$$

$${}^{\bullet}OH + H_2O_2 \rightarrow HO_2^{\bullet} + H_2O \tag{4}$$

$${}^{\bullet}OH + HO_2^{\bullet} \rightarrow H_2O + O_2 \tag{5}$$

The H_2O_2 utilization efficiency was defined as the ratio of the amount of H_2O_2 used to produce 2,3-BDO with the total amount of H_2O_2 consumed in the reaction, as reported by Wang *et al.*[23] As the H_2O_2 dosage increased, the selectivity of acetic acid improved from 3.9% to 44.3%, and the gas products increased slightly from 1.3% to 11.8%; aldehyde did not change evidently. However, the selectivity of 2,3-BDO decreased from 93.1% to 36.5% (Fig. 3A). Furthermore, the H_2O_2 utilization efficiency was reduced from 85.5% to 19.6% with the increase of H_2O_2 concentration (Fig. 3B). Assuming that extensive H_2O_2 was consumed during excessive oxidation or during its self-decomposition the decrease of the utilization efficiency is reasonable. These results are consistent with the conclusion in Fig. 2. When the H_2O_2 quantity is low, the selectivity of 2,3-BDO is high, and the H_2O_2 utilization efficiency is increased. However, the conversion of ethanol is low. Thus, the means to achieve high efficiency in both ethanol conversion and 2,3-BDO formation must be determined.

From the preceding question, we conjectured if 2,3-BDO formation and ethanol conversion could be improved by the successive addition of H_2O_2. The successive addition method may control the local concentration of H_2O_2 through the flow rate to avoid the excessive oxidation of ethanol and the ineffective self-decomposition of H_2O_2. Thus, we compared the

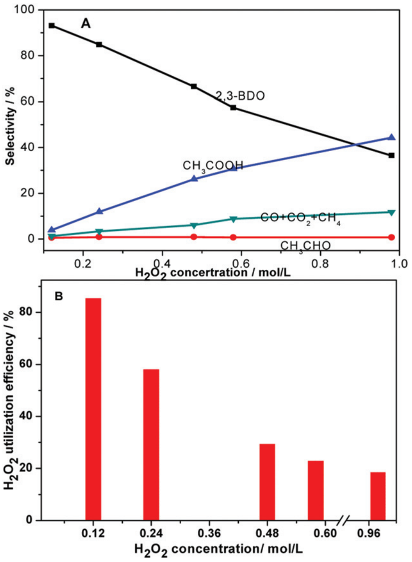

Fig. 3 (A) Effect of the H_2O_2 concentration on the selectivity of products (B) H_2O_2 utilization efficiency as a function of concentration (conditions: 298 K, 5 h, ethanol 0.479 mol, 200 ml; 300 W high pressure Hg lamp).

different addition methods of H_2O_2 through simultaneous and successive addition. The initial concentration of ethanol was 4.8 mol L^{-1}. As shown in Fig. 4A (curve a), the conversion of ethanol increased linearly with the successive addition of H_2O_2 at 2 mL h^{-1} for 5 h. During simultaneous addition (Fig. 4A, curve b), the conversion of ethanol steeply increased at the initial reaction stage and became nearly constant after 5 h. Compared with simultaneous addition, the successive addition method of H_2O_2 improved the ethanol conversion rate from 24.9 mmol h^{-1} to 37.2 mmol h^{-1}, the selectivity of 2,3-BDO from 74.0% to 91.3%, and the utilization efficiency of H_2O_2 from 46.3% to 84.9%. Moreover, for the successive addition of H_2O_2, the selectivity of 2,3-BDO remained basically constant at 91% during the entire irradiation time, and the amounts of aldehyde and acetic acid were minimal (Fig. 4B). The amount of 2,3-BDO formation and ethanol conversion were significantly higher in the successive addition of H_2O_2 than in the simultaneous addition. These results verified that the selective C–H manipulation of bio-ethanol could be achieved successfully by controlling the local H_2O_2 concentration.

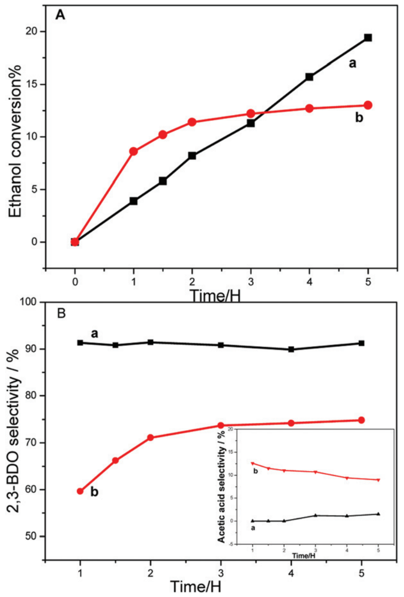

Fig. 4 The effect of the H_2O_2 addition method on ethanol conversion and 2,3-BDO selectivity (curve a: H_2O_2 was added by successive addition at 2 ml h^{-1}; curve b: H_2O_2 was added by simultaneous addition); (reaction conditions: 298 K, ethanol 0.959 mol, H_2O_2 (30%) 0.1 mol, 200 ml; 300 W high pressure Hg lamp).

In order to further enhance the ethanol conversion rate, we consider if it can be achieved *via* accelerating the decomposition of H_2O_2. It was reported that photocatalysts can catalyze H_2O_2 decomposition into $^{\bullet}OH$ by accepting the conduction band electrons, thus we investigated the influence of TiO_2 photocatalysts on the ethanol coupling reaction (entries 2–5, Table 1).[24–26] We found that rutile–TiO_2 can accelerate the decomposition of H_2O_2 to increase the instantaneous concentration of $^{\bullet}OH$ radicals, which improved the ethanol conversion rate from 37.2 mmol h^{-1} to 40.6 mmol h^{-1}. After the Pt cocatalyst was loaded on rutile, the ethanol conversion rate was further enhanced to 47.9 mmol h^{-1}. When using the highly active P25–TiO_2 instead of rutile as the photocatalyst, the ethanol conversion rate can reach the maximum value of 55.1 mmol h^{-1} and the conversion was 31.4%. However, speeding up H_2O_2 decomposition leads to the decrease of 2,3-BDO selectivity and increase of excessive oxide products because of high $^{\bullet}OH$ radical instantaneous concentration (Table S1†). As shown in Fig. S2,† the generation amount of by-products enhanced obviously with the increase of the reaction rate. The improvement of the ethanol conversion rate and maintaining a constant selectivity of 2,3-BDO were contradictory, however, in general, the formation rate of 2,3-BDO can be enhanced by accelerating the reaction rate. For example, the formation rate of 2,3-BDO increased from 15.3 mmol h^{-1} to 18.3 mmol h^{-1} using 0.2% Pt/rutile as the photocatalyst. Thus, controlling and choosing a moderate reaction rate was very important to improve the ethanol conversion rate with a high 2,3-BDO formation rate.

Moreover, based on the decomposition of H_2O_2 catalyzed by ceramic oxides (*e.g.* Al_2O_3 and SiO_2),[27] we investigate the effect of some oxides (*e.g.* SiO_2 nanopowders, SiO_2 mesoporous molecular sieves (SBA-15) and γ-Al_2O_3) on the bio-ethanol coupling reaction (entries 6–8, Table 1). The results were similar to the above rutile-based catalyst, both the ethanol conversion rate and the 2,3-BDO formation rate were improved. In the coupling reaction, γ-Al_2O_3 displayed the highest ethanol conversion rate (55.4 mmol h^{-1}) and the 2,3-BDO formation rate (18.9 mmol h^{-1}). Both the improvement of ethanol conversion and the increase of 2,3-BDO formation rate can be realized successfully by the introduction of a catalyst. In the

Table 1 Experimental data for the photocatalytic C–C coupling of ethanol[a]

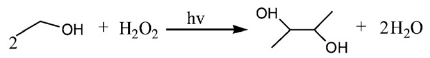

Entry	Catalyst	Ethanol conversion (%)	Conversion rate[b] of ethanol (mmol h^{-1})	2,3-BDO selectivity (%)	Formation rate[c] of 2,3-BDO (mmol h^{-1})
1	No catalyst	19.4	37.2	91.3	15.3
2	Rutile	22.4	40.6	86.1	17.5
3	0.2% Pt/rutile	24.9	44.9	81.4	18.3
4	1% Pt/rutile	26.8	47.9	61.9	14.9
5	1% Pt/P25	31.4	55.1	36.5	10.1
6	SiO_2	25.0	42.4	75.5	16.0
7	SBA-15	27.9	49.6	72.5	18.0
8	γ-Al_2O_3	32.1	55.4	68.6	18.9

[a] Reaction conditions: 298 K, ethanol 0.959 mol, H_2O_2 (30%) 0.1 mol was added by successive addition at 2 ml h^{-1}, 0.2 g of catalyst with 0.2% or 1% of Pt co-catalyst, 200 ml; a 300 W high pressure Hg lamp, 5 h of irradiation time. [b] The rate was calculated on the basis of the converted ethanol. [c] The rate was calculated on the basis of the generated 2,3-BDO.

previous work, Yang *et al.* reported that sacrificial ethanol can be selectively oxidized to 2,3-BDO during the water splitting reaction using Pt/TiO_2 as the photocatalyst, which discovered that the hydroxyl radicals of the TiO_2 surface played an important role in the selective oxidation process. Through fluorine substitution of OH groups of the Degussa P25 surface, the 2,3-BDO selectivity enhanced from approximately 2.6% to approximately 65%.[28] However, this process showed slightly low 2,3-BDO selectivity and requires a long reaction time (24 h). In this work, we utilized directly the $^{\bullet}OH$ radical from the photolysis H_2O_2 to selectively oxidize bio-ethanol to 2,3-BDO, which accelerated the ethanol conversion rate to shorten the reaction time with a relatively high 2,3-BDO selectivity. Moreover, our strategy displayed higher controllability for aliphatic C–H breakage than that reported by Suzuki *et al.*. In a word, this result does not only provide an environment-friendly approach to convert bio-ethanol to 2,3-BDO but also provide a promising channel for selectively manipulating inert aliphatic C–H bonds.

Conclusions

We determined that the α-C–H bond of bio-ethanol could be selectively attacked to achieve a direct C–C coupling synthesis of 2,3-butanediol with hydroxide radicals from the photolysis of H_2O_2 at room temperature. This selective C–H breakage was determined by the reaction rate, which was primarily controlled by the local H_2O_2 concentration at a given irradiation intensity. The low local H_2O_2 concentration was favorable for selectively cleaving the α-C–H bond of alcohols. At a moderate reaction rate of ethanol (37 mmol h^{-1}), the 2,3-butanediol selectivity could reach 91%. The introduction of a catalyst can further increase the ethanol conversion rate from 37.2 mmol h^{-1} to 55.4 mmol h^{-1} and enhance the formation rate of 2,3-BDO from 15.3 mmol h^{-1} to 18.9 mmol h^{-1} *via* accelerating H_2O_2 decomposition. In comparison with the previous synthetic method of 2,3-BDO, our strategy displays a shorter reaction time, higher 2,3-BDO selectivity and faster ethanol conversion rate. This approach is a rational strategy to manipulate a single bond selectively in alcohols and to help explain C–C formation in natural photosynthesis.

Experimental section

All chemical reagents were analytical grade reagents and used without further purification. SiO_2 nanopowders (15 nm, 99.5%) and γ-Al_2O_3 (40–60 mesh) were purchased from Aladdin. Particle surface areas were determined on a Quantachrome Autosorb 1 analyzer using nitrogen adsorption and desorption at equilibrium vapor pressure and the Brunauer–Emmet–Teller (BET) method of surface area calculation. Specific surface areas of SiO_2 nanopowders, SiO_2 mesoporous molecular sieves (SBA-15) and γ-Al_2O_3 particles were 124.3, 712.0 and 209.6 m^2 g^{-1}, respectively. The adsorption average pore diameter of SiO_2 nanopowders, SBA-15 and γ-Al_2O_3 particles were 11.2, 5.52 and 8.24 nm, respectively.

Rutile–TiO_2 was synthesized by a calcination method with commercial TiO_2 powder in a muffle furnace in air at 800 °C for 8 h. SBA-15 was synthesized according to the method reported elsewhere.[29]

Photochemical experiments were conducted in a 250 mL inner irradiation-type Pyrex reactor. A 300 W high-pressure mercury vapor lamp was used as the incandescent light source and was cooled by water to maintain the reactions at room temperature. All the photochemical tests were performed in a 200 mL aqueous solution of reactants and were magnetically stirred to achieve full dispersion, with pure Ar continuously bubbling. Before the photochemical reaction, Ar was purged into the reactor for 30 min to remove the air thoroughly. The reaction course was monitored by periodically sampling the liquid and gas from a sampling valve. Liquid samples were analyzed using a gas chromatograph (Haixin; GC-950) equipped with a flame ionization detector (FID). Gaseous samples were analyzed using a gas chromatograph (Fuli;

GC-9790) equipped with a thermal conductivity detector (TCD), a FID. Quantities of the products and reactants were calculated from the peak areas of the compounds using calibration curves.

All the photocatalytic tests were carried out using 0.2 g of catalyst and 200 mL of 0.959 mol ethanol aqueous solution and H_2O_2 (30%) (0.1 mol) was added by using a peristaltic pump at 2 ml h^{-1} over 5 h followed by an appropriate amount (0.2% and 1% Pt) of chloroplatinic acid ($H_2PtCl_6{\cdot}6H_2O$). Before the photocatalyst reaction, Ar was purged into the reactor for 30 min to remove the air thoroughly. The other reaction course was similar to the above photochemical experiment.

EPR spectra were recorded using a Bruker EMXplus-10/12. The typical parameters were as follows: sweep width = 100 G, EPR microwave power = 10 mW, modulation amplitude = 0.8 G, time constant = 40.96 ms, and sweep time = 167.77 s. The values of the g-tensor were calculated using Bruker's WIN-EPR SimFonia 2.3 program, which allowed the control of the Bruker EPR spectrometer, data acquisition, automation routines, tuning, and calibration programs on a PC with a Windows operating system. The exact *g*-values of the key spectra were determined by comparing with the 2,2-diphenyl-1-picrylhydrazyl (DPPH) standard.

Acknowledgements

This research was financially supported by the National Natural Science Foundation of China (21173250 and U1510108) and the Knowledge Innovation Project of the Chinese Academy of Sciences (KGCX2-EW-311).

Notes and references

1 Y. Y. Ma, Z. T. Du, J. X. Liu, F. Xia and J. Xu, *Green Chem.*, 2015, **17**, 4968–4973.

2 Y. Yan, P. Feng, Q. Z. Zheng, Y. F. Liang, J. F. Lu, Y. Cui and N. Jiao, *Angew. Chem., Int. Ed.*, 2013, **52**, 5827–5831.

3 T. Patra, R. Watile, S. Agasti, T. Naveen and D. Maiti, *Chem. Commun.*, 2016, **52**, 2027–2030.

4 E. M. Simmons and J. F. Hartwig, *Nat. Lett.*, 2012, **483**, 70–73.

5 J. R. Hansen, C. H. Christensen, J. Sehested, S. Helveg, J. R. R. Nielsen and S. Dahl, *Green Chem.*, 2007, **9**, 1016–1021.

6 D. P. Ho, H. H. Ngo and W. Guo, *Bioresour. Technol.*, 2014, **169**, 742–749.

7 M. Samei, T. Mohammadi and A. A. Asadi, *Chem. Eng. Res. Des.*, 2013, **91**, 2703–2712.

8 M. R. Ladisch and K. Dyck, *Science*, 1997, **205**, 898–900.

9 J. F. DeWilde, C. J. Czopinski and A. Bhan, *ACS Catal.*, 2014, **4**, 4425–4433; C. Bianchini and P. K. Shen, *Chem. Rev.*, 2009, **109**, 4183–4206; T. K. Phung and G. Busca, *Chem. Eng. J.*, 2015, **272**, 92–101; T. K. Phung and G. Busca, *Catal. Commun.*, 2015, **68**, 110–115.

10 R. G. Zhang, Z. X. Liu, L. X. Ling and B. J. Wang, *Appl. Surf. Sci.*, 2015, **353**, 150–157.

11 S. Hanspal, Z. D. Young, H. Shou and R. J. Davis, *ACS Catal.*, 2015, **5**, 1737–1746.

12 A. B. Śanchez, N. Homs, S. Miachon, J. A. Dalmon, J. G. Fierrodand and P. R. Piscina, *Green Chem.*, 2011, **13**, 2569–2575.

13 M. Kopke, C. Mihalcea, F. Liew, J. H. Tizard, M. S. Ali, J. J. Conolly and S. D. Simpson, *Appl. Environ. Microbiol.*, 2011, **77**, 5467–5475.

14 X. J. Ji, H. Huang and P. K. Ouyang, *Biotechnol. Adv.*, 2011, **29**, 351–364.

15 J. V. Haveren, E. L. Scott and J. Sanders, *Biofuels, Bioprod. Biorefin.*, 2008, **2**, 41–57.

16 S. Hrivastav, J. Lee, H. Y. Kim and Y. R. Kim, *J. Microbiol. Biotechnol.*, 2013, **23**, 885–896.

17 C. F. Huang, Y. F. Jiang, G. L. Guo and W. S. Hwang, *Bioresour. Technol.*, 2013, **135**, 446–453.

18 T. W. Yang, Z. M. Rao, X. Zhang, M. J. Xu, Z. H. Xu and S. T. Yang, *Appl. Microbiol. Biotechnol.*, 2013, **97**, 7651–7658.

19 S. Hrivastav, J. Lee, H. Y. Kim and Y. R. Kim, *J. Microbiol. Biotechnol.*, 2013, **23**, 885–896.

20 S. Kim, S. O. Seo, Y. C. Park, Y. S. Jin and J. H. Seo, *J. Biotechnol.*, 2014, **192**, 376–382.

21 X. X. Wang, H. Y. Hu, D. H. Liu and Y. Q. Song, *New Biotechnol.*, 2016, **1**, 16–22.

22 Y. Shimizu, S. Sugimoto, S. Kawanishi and N. Suzuki, *Bull. Chem. Soc. Jpn.*, 1991, **64**, 3607–3612.

23 W. G. Li, Y. Wang and A. Irinic, *Chem. Eng. J.*, 2014, **244**, 1–8.

24 J. G. Jia, T. Ohno and M. Matsumura, *Chem. Lett.*, 2000, 908–909.

25 B. L. Tang, G. H. Jiang, Z. Wei, X. Li, X. H. Wang, T. T. Jiang, W. X. Chen and J. M. Wan, *Acta Metall. Sin.*, 2014, **27**, 124–130.

26 C. F. Yu, S. Y. Dong, J. L. Feng, J. Y. Sun, L. M. Hu, Y. K. Li and J. H. Sun, *Environ. Sci. Pollut. Res.*, 2014, **21**, 2837–2845.

27 A. Hiroki and J. A. LaVerne, *J. Phys. Chem. B*, 2005, **109**, 3364–3370.

28 P. J. Yang, J. H. Zhao, B. Y. Cao, L. Li, Z. J. Wang, X. X. Tian, S. P. Jia and Z. P. Zhu, *ChemCatChem*, 2015, **7**, 2384–2390.

29 L. N. Zhang, H. Wang, Z. F. Qin, J. G. Wang and W. B. Fan, *RSC Adv.*, 2015, **5**, 22838–22846.